RESEARCH ARTICLE

Figures and figure supplements

Bidirectional regulation of glial potassium buffering – glioprotection versus neuroprotection

Hailun Li *et al*

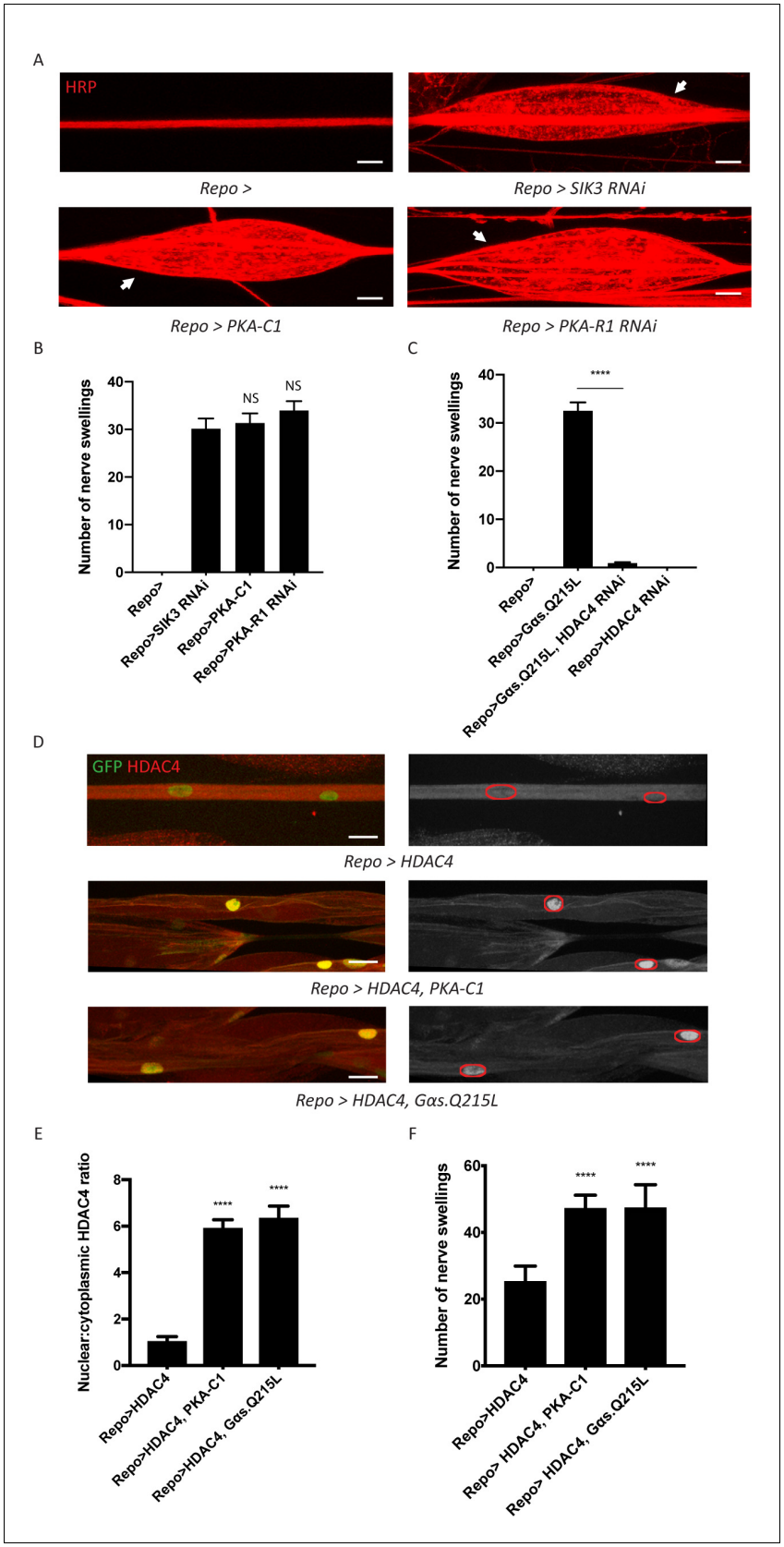

Figure 1. A G-protein-coupled receptor-protein kinase A (GPCR-PKA) signaling axis regulates salt inducible kinase 3 (SIK3)-mediated glial K^+ buffering. (**A**) Representative images of larval peripheral nerves stained for the nerve

Figure 1 continued on next page

Figure 1 continued

membrane marker HRP. Repo-GAL4, a pan-glial driver, was used to express LexA RNAi (control; abbreviated as *Repo>*), SIK3 RNAi (*Repo>SIK3 RNAi*), PKA-R1 RNAi (*Repo>PKA-R1 RNAi*), or a UAS-PKA-C1 transgene (*Repo>PKA-C1*). PKA hyperactivity, induced by either glial overexpression of its catalytic subunit (PKA-C1) or knockdown of a regulatory subunit (PKA-R1), causes localized nerve swellings (arrow) that resemble defects caused by loss of SIK3 from glia. Control larvae do not display swellings. Scale bars 20 μm. (**B**) Quantification of nerve swellings in (**A**). n ≥ 30. One-way ANOVA with Tukey's multiple comparisons; NS = not significant, p>0.05. (**C**) Quantification of nerve swellings per animal in control, larvae with glial expression of constitutively activated Gαs protein, HDAC4 RNAi, or co-expression of HDAC4 RNAi and Gαs. Constitutively activated Gαs in glia (*Repo>$G_s\alpha$. Q215L*) causes nerve swellings that resemble (**A**); swellings are suppressed by loss of HDAC4 from glia (*Repo>$G_s\alpha$. Q215L, HDAC4 RNAi*). Glial knockdown of HDAC4 (*Repo>HDAC4 RNAi*) does not result in nerve swellings. n ≥ 30. One-way ANOVA with Tukey's multiple comparisons; ****, p<0.0001. (**D**) Representative images of larval peripheral nerves demonstrating the effects of Gαs and PKA activation on HDAC4 localization in glia. Left: glial nuclei (green) and HDAC4 (red). Right: grayscale images show HDAC4 staining; glial nuclei are outlined. Scale bars 15 μm. (**E**) Quantification of nucleo:cytoplasmic ratio of HDAC4 for genotypes in (**D**). n ≥ 20. Data are presented as fold changes relative to *Repo>HDAC4*. One-way ANOVA with Tukey's multiple comparisons; ****, p<0.0001. (**F**) Quantification of number of nerve swellings per animal for genotypes in (**D**). n ≥ 20. One-way ANOVA with Tukey's multiple comparisons; ****, p<0.0001. Data are mean ± SEM.

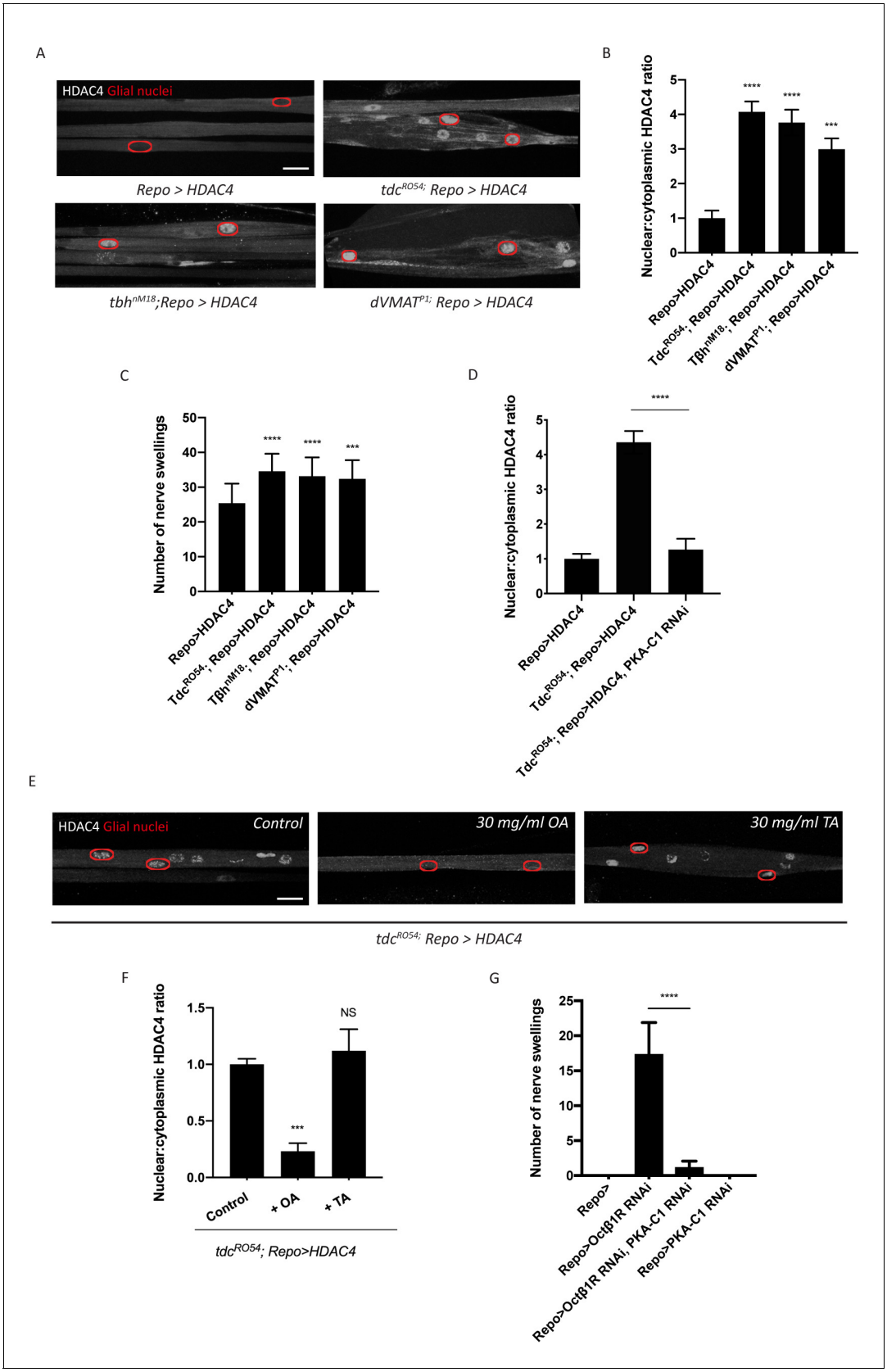

Figure 2. Octopamine is required to activate salt inducible kinase 3 (SIK3)-regulated K^+ buffering program in glia. (**A**) Representative images of peripheral nerves showing aberrant HDAC4 localization in octopamine synthesis and transport mutants. Grayscale images show HDAC4 staining; glial

Figure 2 continued on next page

Figure 2 continued

nuclei are outlined in red. Scale bars 15 μm. (**B**) Quantification of nucleo:cytoplasmic ratio of HDAC4 for genotypes in (**A**). n ≥ 20. Data are presented as fold changes relative to *Repo>HDAC4.* One-way ANOVA with Tukey's multiple comparisons; ***, p<0.001; ****, p<0.0001. (**C**) Quantification of number of nerve swellings per animal in HDAC4 overexpressing control larvae (*Repo>HDAC4*) and octopamine mutants. n ≥ 20 larvae per genotype. One-way ANOVA with Tukey's multiple comparisons; ***, p<0.001. ****, p<0.0001. (**D**) Quantification of HDAC4 localization in octopamine synthesis mutants, mutants with glial expression of LexA RNAi as control or PKA-C1 RNAi. Octopamine synthesis mutants (*tdc2^{RO54}*) exhibit HDAC4 accumulation in glial nuclei; this nuclear localization is rescued by abolishing protein kinase A (PKA) catalytic activity in glia (*Repo>PKA-C1 RNAi*). One-way ANOVA with Tukey's multiple comparisons; ****, p<0.0001. (**E**) Representative images of nerves demonstrating the effect of 30 mg/ml octopamine or 30 mg/ml tyramine on octopamine synthesis mutant glia in an ex vivo assay. Scale bars 15 μm. (**F**) Quantification of HDAC4 nucleo:cytoplasmic ratio for genotypes in (**D**). Octopamine (30 mg/ml), but not TA (30 mg/ml) or KCl (500 mM), suppresses HDAC4 nuclear localization in glia. n ≥ 15. One-way ANOVA with Tukey's multiple comparisons; ***, p<0.001; NS = not significant, p>0.05. (**G**) Quantification of number of nerve swellings per animal in larvae with glial expression of LexA RNAi as control (*Repo>*), Octβ1R RNAi, PKA-C1 RNAi, or co-expression of Octβ1R RNAi and PKA-C1 RNAi. n ≥ 20. Student's t test; ****, p<0.0001. Data are mean ± SEM.

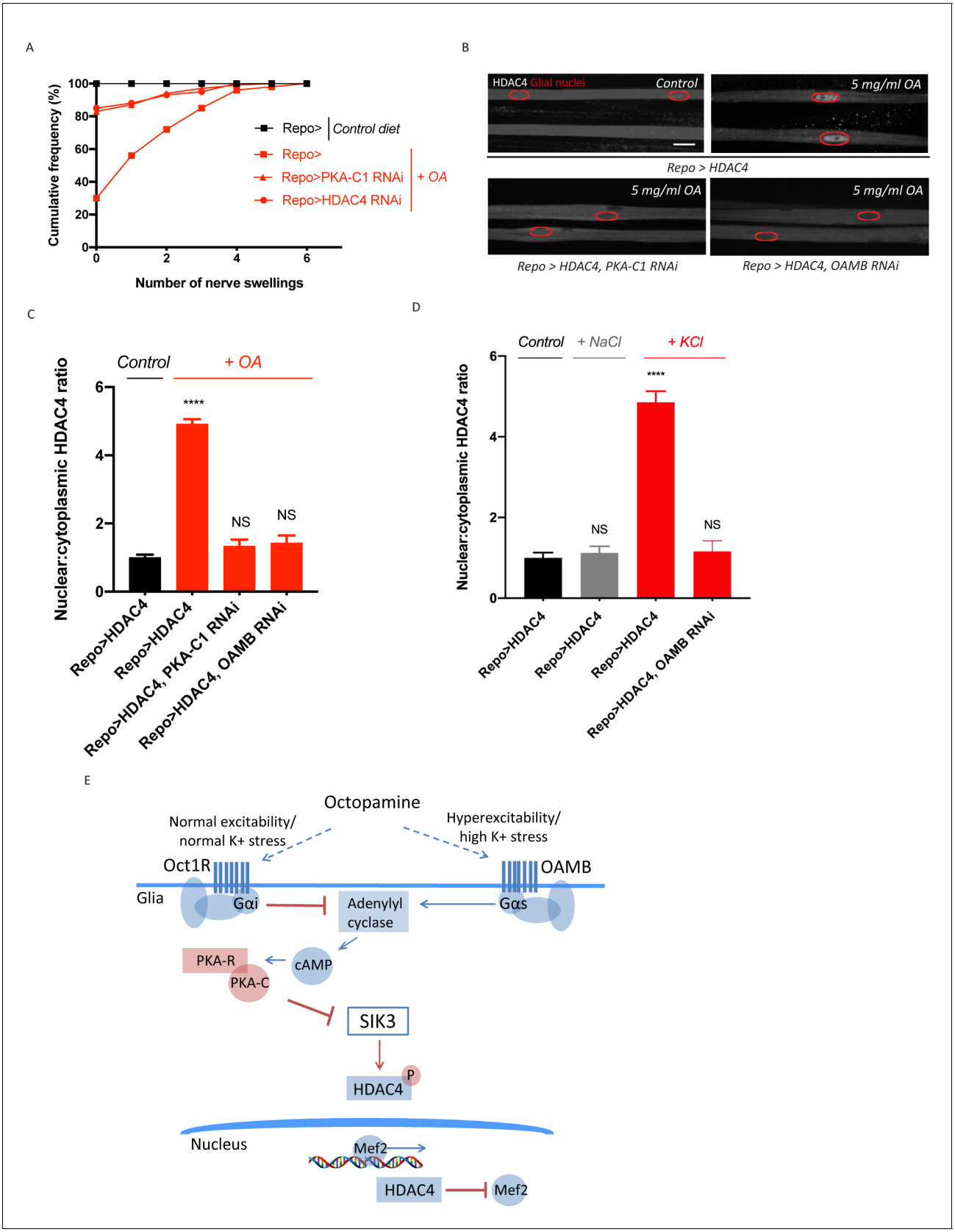

Figure 3. Excess octopamine inhibits salt inducible kinase 3 (SIK3) signaling to downregulate glial K^+ buffering. (**A**) Frequency of occurrence of nerve swellings in high octopamine-fed larvae with glial expression of LexA RNAi (*Repo>*), PKA-C1 RNAi, or HDAC4 RNAi. Larvae raised on control diet do

Figure 3 continued on next page

Figure 3 continued

not develop swellings; high octopamine (5 mg/ml) diet, but not high TA (5 mg/ml) diet, increases the percent of larvae exhibiting nerve swellings; this effect is blocked by loss of PKA-C1 or HDAC4 from glia. n ≥ 100. (**B**) Representative images of peripheral nerves demonstrating the effect of high octopamine diet on glial HDAC4 localization. High octopamine diet enhances HDAC4 nuclear localization in control larvae (*Repo>HDAC4*); this effect is blocked by glial knockdown of PKA-C1 (*Repo> PKA-C1 RNAi*) or OAMB (*Repo>OAMB RNAi*). Grayscale images show HDAC4 staining; glial nuclei are outlined in red. Scale bars 15 μm. High octopamine diet promotes nuclear localization of HDAC4 specifically in wrapping glia, as shown in ***Figure 3—figure supplement 1***. (**C**) Quantification of HDAC4 nucleo:cytoplasmic ratio for genotypes in (**B**). n ≥ 30. Data are presented as fold changes relative to *Repo>HDAC4*. One-way ANOVA with Tukey's multiple comparisons; ****, p<0.0001. NS = not significant, p>0.05. (**D**) Quantification of HDAC4 localization in larvae raised on high salt diets. KCl-rich (200 mM) diet, but not NaCl-rich (200 mM) diet, promotes nuclear shuttling of HDAC4 in control larvae (*Repo>HDAC4*); this re-localization is inhibited by glial knockdown of OAMB (*Repo>OAMB RNAi*). n ≥ 20. One-way ANOVA with Tukey's multiple comparisons; ****, p<0.0001; NS, p>0.05. (**E**) Schematic model of octopamine exerting dual effects on SIK3-mediated glial K^+ buffering: in response to K^+ stress, different levels of octopamine act through receptors with antagonistic functions to differentially regulate SIK3-mediated glial K^+ buffering. Data are mean ± SEM.

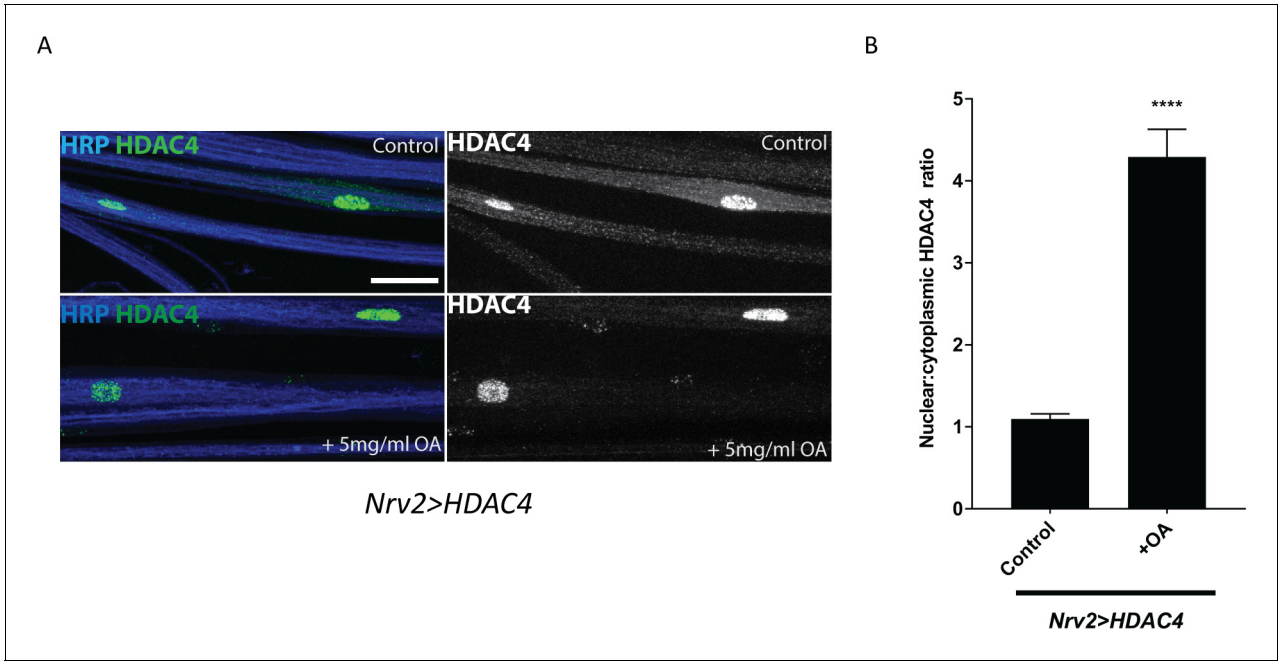

Figure 3—figure supplement 1. Excess octopamine in wrapping glia downregulates glial K^+ buffering. (**A**) Representative images of peripheral nerves showing HDAC4 localization in wrapping glia (Nrv2>HDAC4) of larvae raised on a normal or a high-octopamine diet. High octopamine leads to a high nucleo:cytoplasmic ratio of HDAC4. Grayscale images show HDAC4 staining. Scale bars 15 µm. (**B**) Quantification of HDAC4 nucleo:cytoplamic ratio for genotypes in (**A**). n ≥ 12. Data are presented as fold changes relative to *Nrv2*>HDAC4 + normal diet. Student's t test; ****, p<0.0001.

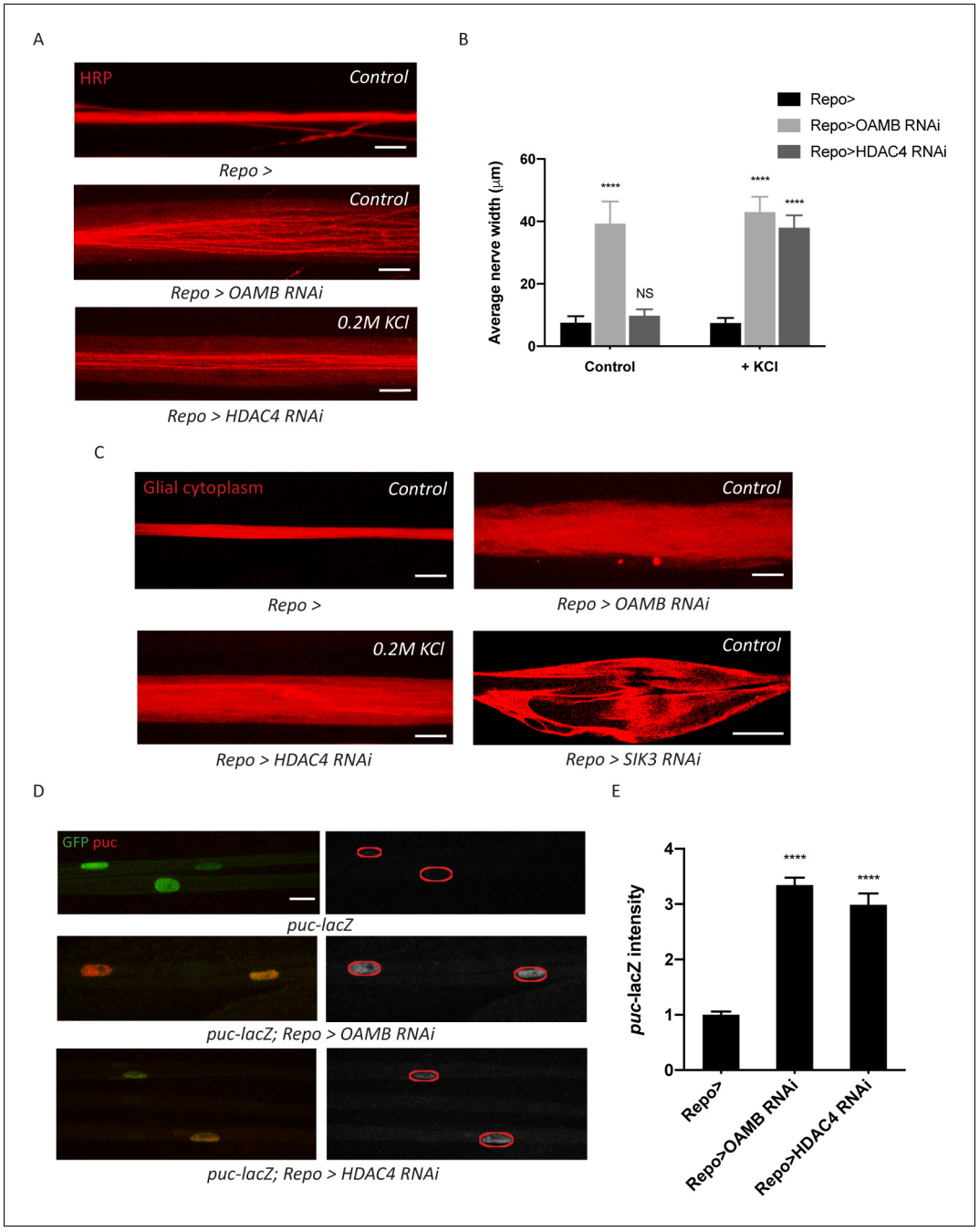

Figure 4. Glia with enhanced K^+ buffering capacity undergo swelling and stress responses. (**A**) Representative images of HRP-stained peripheral nerves demonstrating 'non-localized' edema in larvae with glial expression of LexA RNAi (*Repo>*), OAMB RNAi, or HDAC4 RNAi. Scale bars 20 μm. (**B**) Quantification of average nerve width for genotypes in (**A**). Loss of OAMB from glia causes 'non-localized' edema that results in a uniform increase in nerve width along the entire nerve; HDAC4 knockdown in glia induces a similar phenotype when larvae were fed a KCl-rich (200 mM) diet. n ≥ 15. Two-way ANOVA with Tukey's multiple comparisons; ****, p<0.0001; NS = not significant, p>0.05. (**C**) Representative thin optical sections of larval peripheral nerves with RFP-labeled (red) glial cytoplasm. (**D**) Representative images of larval peripheral nerves stained for c-Jun N-terminal kinase (JNK) pathway activity reporter *puc-lacZ*. Left: glial nuclei (green) and puc (red). Right: grayscale images show puc-lacZ staining; glial nuclei are outlined. Scale bars 15 μm. (**E**) Quantification of puc-lacZ signals in glia for genotypes in (**C**). Loss of OAMB or HDAC4 from glia dramatically increases *puc* expression in glia. n ≥ 20. One-way ANOVA with Tukey's multiple comparisons; ****, p<0.0001. Data are presented as fold changes relative to *puc-lacZ; Repo>*. Data are mean ± SEM.

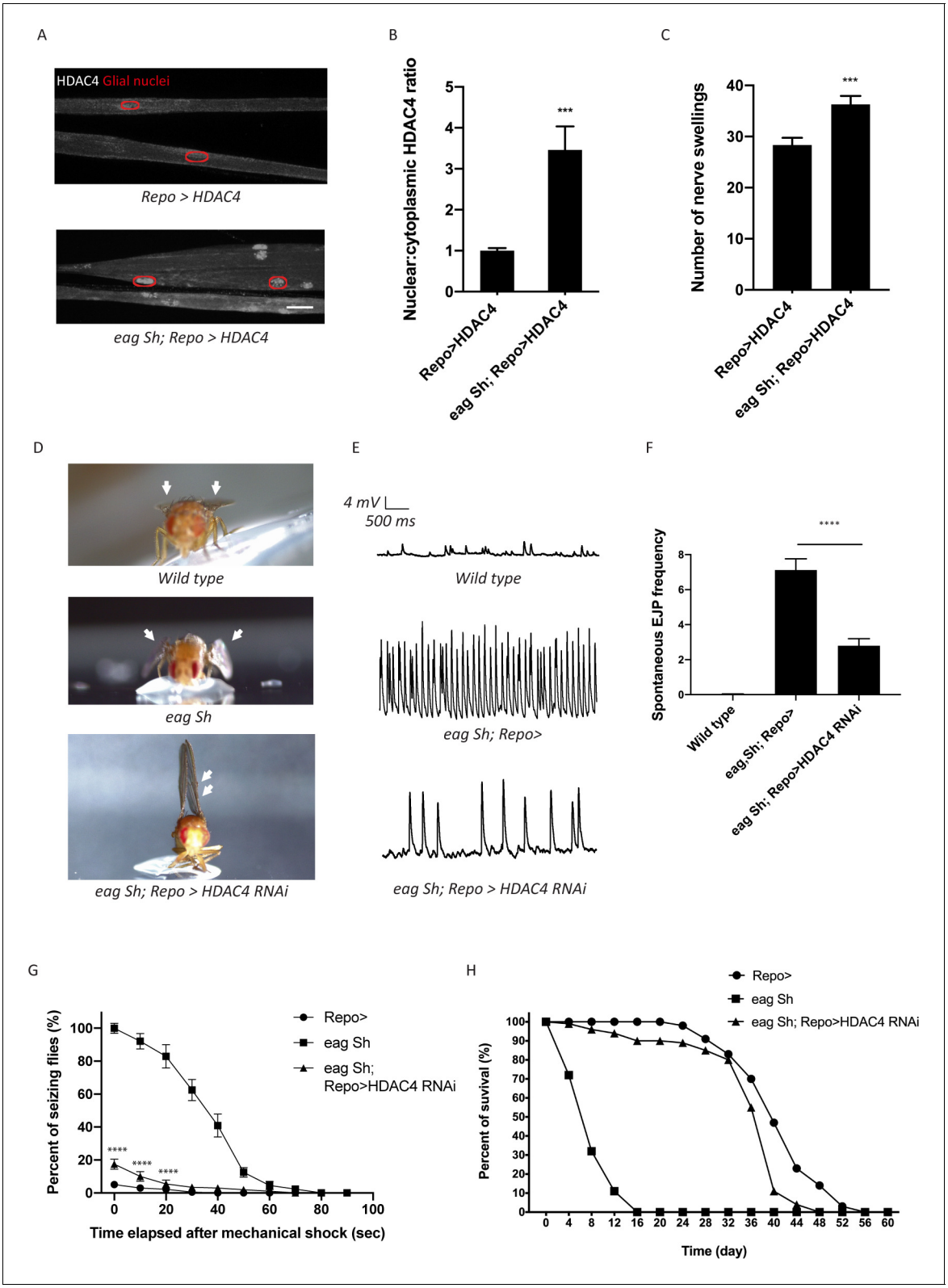

Figure 5. Enhanced glial K^+ buffering suppresses hyperexcitability in *eag,Sh* mutant. (**A**) Representative images of peripheral nerves demonstrating aberrant HDAC4 localization in *eag,Sh* mutant. Grayscale images show HDAC4 staining; glial nuclei are outlined in red. Scale bars 15 µm. (**B**) Quantification of HDAC4 nucleo:cytoplasmic ratio for genotypes in (**A**). n ≥ 20. Data are presented as fold changes relative to *Repo>HDAC4.* Student's t test; ***, p<0.001. (**C**) Quantification of nerve swellings in HDAC4-overexpressing control and eag shaker mutant. n ≥ 20. Student's t test; ***,

Figure 5 continued on next page

Figure 5 continued

p<0.001. (**D**) Representative images of wing morphology in control, *eag,Sh* mutants, and mutants with glial knockdown of HDAC4. *Eag,Sh* mutants exhibit down-turned wings (arrow) that are not observed in control flies; this phenotype is suppressed by glial-specific inhibition of HDAC4 (*Repo>HDAC4 RNAi*). (**E**) Representative physiological traces recorded from larval neuromuscular junctions (NMJs) for genotypes in (**D**). Control larvae (*Repo>*) only exhibit miniature excitatory junction potentials (mEJPs); *eag,Sh* exhibit spontaneous evoked junction potentials (EJPs). These spontaneous EJPs are suppressed by glial expression of HDAC4 RNAi. (**F**) Quantification of frequency of spontaneous EJPs for genotypes in (**D**). A minimum of 50 consecutive events were analyzed over a passive recording window (up to 75 consecutive events or 120 s, whichever happened first), and events with amplitudes ≥4 mV were considered as spontaneous EJPs. n = 8 for *Repo>*; n = 8 for *eag,Sh*; n = 8 for *eag,Sh; Repo>HDAC4 RNAi*. One-way ANOVA with Tukey's multiple comparisons; p<0.0001. (**G**) Time course of vortex-induced seizure behaviors for genotypes in (**D**). n ≥ 5 groups of 10 flies per genotype per time point. Two-tailed Student's t test; ****, p<0.0001. (**H**) Life span analysis of genotypes in (**D**). n ≥ 50. Data are mean ± SEM.